Composition dependent properties of Fe_3Si films grown on GaAs(113)*A* substrates

P. K. Muduli,[a] K.-J. Friedland, J. Herfort, H.-P. Schönherr, and K. H. Ploog
Paul-Drude-Institut für Festkörperelektronik, Hausvogteiplatz 5-7, D-10117 Berlin, Germany

(Presented 13 November 2008; received 17 September 2008; accepted 27 November 2008; published online 5 March 2009)

Structural, electrical, and magnetic properties of Fe_3Si/GaAs(113)*A* hybrid structures are studied, dependent on the layer composition varying from 15 to 26 at. % Si. The presence of superlattice reflections in x-ray diffraction and lower resistivity confirms the long-range atomic ordering in the stoichiometric Fe_3Si films, reflecting the $D0_3$ crystal structure. The observed atomic ordering is also found to influence the sign and magnitude of the antisymmetric component of the planar Hall effect observed in this orientation. However a finite disorder is observed even in nearly stoichiometric samples. © *2009 American Institute of Physics*. [DOI: 10.1063/1.3072832]

Ferromagnet/semiconductor heterostructures are important for spin-electronic devices.[1] In order to achieve higher spin injection efficiency, the interface structure between the semiconductor and ferromagnet must be controlled carefully.[2] This is often performed by careful low temperature growth and processing. Growth or postgrowth annealing at modest temperatures can lead to interdiffusion and the formation of some interfacial compounds. For Fe or Co on GaAs, interaction and interdiffusion occur at moderate temperatures of about 200 °C.[3] Therefore, it is highly desirable to obtain alternative ferromagnets that show improved interfacial quality as well as a higher thermal stability. Fe_3Si is one such alternative material that exhibits better thermal stability[4,5] compared to Fe and other elemental ferromagnets. It is known to be ferromagnetic up to 840 K, and it has a cubic $D0_3$ crystal structure with a lattice constant of 5.653 Å, which is close to the lattice constant of GaAs. It is also regarded as a Heusler alloy, which is a promising candidate for spintronic applications due to its high Curie temperatures of 200–1100 K and its high degree of spin polarization[6] though calculated density of states for bulk Fe_3Si does not predict a half-metallic behavior.[7] For these reasons, Fe_3Si films epitaxially grown on semiconducting substrates such as GaAs (Refs. 8–11) and Si (Refs. 12 and 13) have promoted strong interests recently. Another striking advantage of Fe_3Si is the easy growth control compared to complex ternary Heusler alloys. This is not only due to its binary nature but also due to the broad phase stability of the Fe_3Si alloy, with Si contents ranging from 9.5 to 26 at. % Si.[14]

In this work, we present a study of the structural, electrical, and magnetic properties of Fe_3Si/GaAs(113)*A* hybrid structures dependent on the layer composition, with special focus on the influence of atomic ordering on these properties. Here we have chosen the GaAs(113)*A* surface, which is characterized by a low-surface symmetry, as the substrate for the growth of Fe_3Si films. Due to this low-surface symmetry, a unique antisymmetric contribution to the planar Hall effect (PHE) in the Fe(113) and Fe_3Si(113) films has been observed.[15] We will show that this antisymmetric component exhibits a sensitive dependence on atomic ordering. The properties will be compared with the Fe_3Si films grown on the GaAs(001) substrates.[8,10,11]

The high quality Fe_3Si films are grown on GaAs(113)*A* substrates by molecular-beam epitaxy.[9] The structural and crystalline qualities of these $Fe_{3+x}Si_{1-x}$ films show smooth surface morphology as well as a sharp interface with GaAs, as discussed elsewhere.[9] The high resolution x-ray diffraction (HRXRD) measurements are performed *ex situ* with a PANalytical X'pert diffractometer using Cu $K\alpha$ radiation with a Ge(220) monochrometer and a triple-bounce analyzer crystal. The magnetic properties of these films are studied *ex situ* using a commercial Quantum Design MPMS XL superconducting quantum interference device magnetometry. The transport measurements are performed on layers with lithographically patterned Hall bars aligned along the $[33\bar{2}]$ direction. The width of the Hall bar is 30 μm, and the separation between the voltage leads is 22.5 μm.

The cubic $D0_3$ structure of Fe_3Si is considered as four interpenetrating fcc sublattices *A*, *B*, *C*, and *D* with origins at $A(0,0,0)$, $B(0.25,0.25,0.25)$, $C(0.5,0.5,0.5)$, and $D(0.75,0.75,0.75)$. In the ordered Fe_3Si crystal, Fe atoms occupy the three sublattices *A*, *B*, and *C*, while Si atoms fill the sublattice *D*. In HRXRD measurements, Bragg reflections for this structure are obtained for planes with either all odd or all even Miller indices (h,k,l). The reflections for which *h*, *k*, and *l* are all even with $(h+k+l)=4n$ are fundamental reflections and are unaffected by the state of ordering. The reflections for which *h*, *k*, and *l* are all even with $(h+k+l)=4n+2$ are sensitive to an $(A,C)\leftrightarrow D$ disorder, whereas the reflections with odd *h*, *k*, and *l* are sensitive to both $B\leftrightarrow D$ and $(A,C)\leftrightarrow D$ disorder.[16,17] The relative intensities of these two classes of superlattice reflections depend on the state of ordering. But for a perfectly ordered lattice, the intensities should be equal.[16] For example, the (002) and (113) reflections should have the same intensity for a perfectly ordered Fe_3Si lattice. Hence to investigate the atomic

[a]Electronic mail: muduli@kth.se. Present address: Department of Microelectronics and Applied Physics, Royal Institute of Technology, Electrum 229, 164 40 Kista, Sweden.

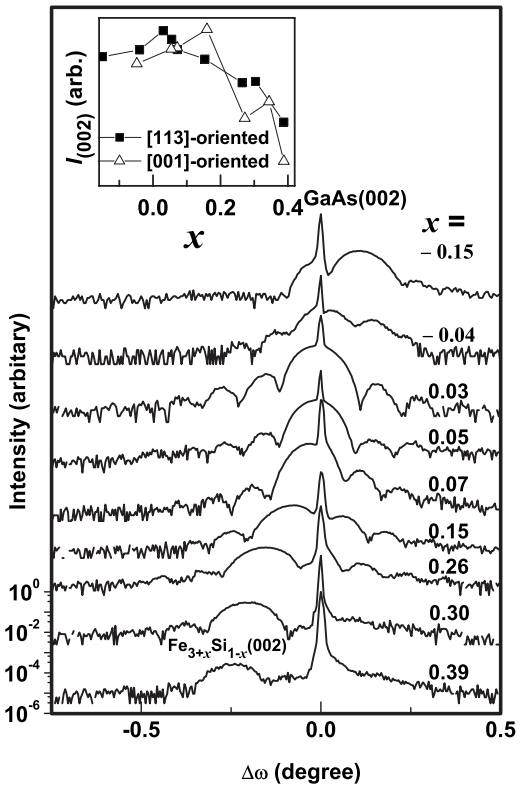

FIG. 1. Normalized *skew-symmetric* ω-2θ scans of Fe_3Si/GaAs(113)*A* near the superlattice (002) reflection. The curves are normalized to the GaAs(002) reflection and are shifted with respect to each other for clarity. The inset shows a plot of intensity of (002) reflection $I_{(002)}$ as a function of the composition x for [113]- and [001]-oriented films.

ordering of the Fe_3Si films, we analyze these two different superlattice reflections. The results are summarized in Figs. 1 and 2 as a function of composition x of the $Fe_{3+x}Si_{1-x}$ films, where x denotes the deviation from stoichiometry.

We found an increase in the intensity of the (002) reflection with increasing Si content toward stoichiometry, as shown in Fig. 1. This is more clearly seen in the inset in Fig.

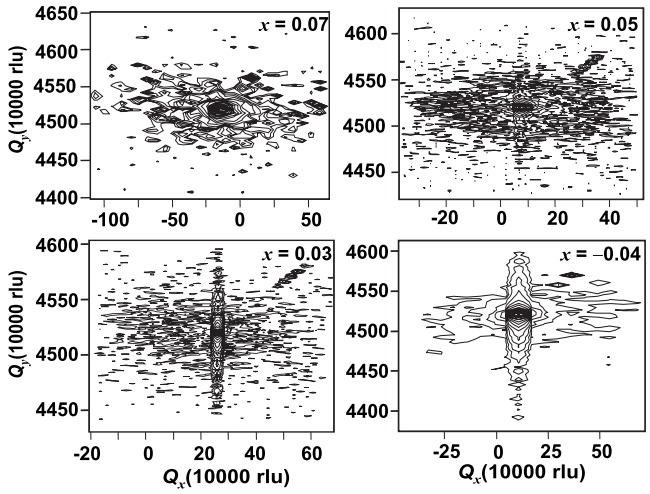

FIG. 2. X-ray reciprocal space maps of stoichiometric Fe_3Si films grown on GaAs(113)*A* substrates for the symmetric and superlattice (113) reflection. The reciprocal lattice unit (rlu) is $\lambda/2d$, where λ is the wavelength of Cu $K\alpha 1$ radiation and d is the lattice plane spacing of the corresponding reflection.

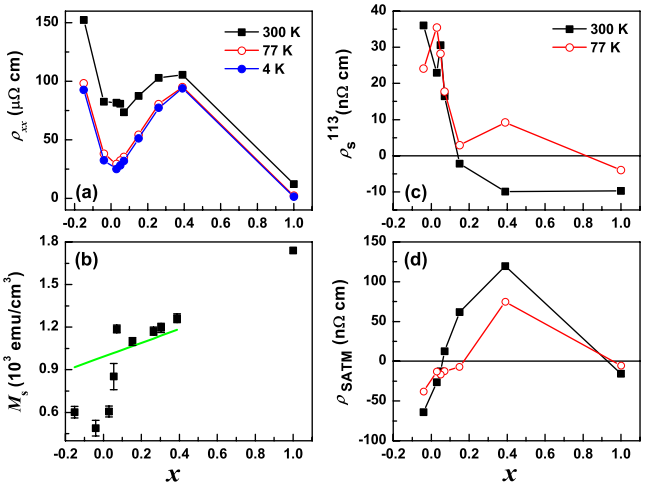

FIG. 3. (Color online) (a) Resistivity ρ_{xx} as a function of composition x for the $Fe_{3+x}Si_{1-x}$ alloys at 300, 77, and 4 K. (b) Saturation magnetization M_s as a function of composition x. Open rectangles are experimental points, whereas the solid line is the behavior according to Eq. (2). Composition dependence of the (c) symmetric PHE amplitude ρ_s^{113} and (d) antisymmetric amplitude ρ_{SATM} obtained from the fitting of transverse resistivity at a saturating field. In these figures $x=1$ represents a 20-nm-thick Fe film grown on GaAs(113)*A* substrates.

1, where intensity $I_{(002)}$ of the (002) layer reflection is plotted as a function of composition. The substrate reflection GaAs(002) is used as a reference to scale the intensity $I_{(002)}$. For comparison, the intensities of the Fe_3Si/GaAs(001) films are also shown. The behavior for both orientations is qualitatively similar, though in some cases, [113]-oriented samples exhibit slightly higher $I_{(002)}$. The superlattice and symmetric (113) reflections with odd h, k, and l are detectable only for the most stoichiometric samples with $x=0.05$, 0.03, and -0.04, as shown in Fig. 2. A slight increase in the intensity of the (113) reflection is also observed from $x=0.05$ to -0.04. Here, we show reciprocal space maps around the (113) reflection since the layer peak was not detected in normal symmetric ω-2θ scans. In Fig. 2, the distinction of the layer peak from the substrate peak (for $x=0.05$, 0.03, and -0.04) is not very clear. This is because the GaAs(113) reflection itself is rather broad and the layer peak is very close to that of the substrate peak. However, the interface fringes can be identified from the elongation along Q_y, indicating the presence of the layer reflection. Thus we observe an improvement in the long-range ordering of the lattice with increasing Si content toward stoichiometry. The observation of the (002) and (113) superlattice reflections for the nearly stoichiometric samples indicates the formation of the $D0_3$ crystal structure. However, the intensity of the (113) reflection of the layer was found lower compared to the (002) reflection in all samples, indicating a finite disorder even in the nearly stoichiometric samples.[11]

The effect of atomic ordering on electrical and magnetic properties is discussed in Fig. 3. For all studied temperatures, the resistivity ρ first increases with increasing Si content until $x=0.3$. However with further increase in the Si content, ρ shows a strong decrease, and a minimum is reached around the stoichiometry. For even higher Si contents ρ increases again. This behavior is very similar to that in bulk,[18]

$Fe_3Si(001)$ films[19] and can be understood from the Fe-Si site disorder. The electrical resistivity to a first approximation is given by:

$$\rho_{xx}(T) = \rho_0 + \rho_p(T), \tag{1}$$

where ρ_0 is the temperature independent residual resistivity due to impurity or alloy scattering mechanisms and $\rho_p(T)$ is the temperature dependent resistivity due to scattering by phonons. The residual resistivity ρ_0 is assumed to be temperature independent. In $Fe_{3+x}Si_{1-x}$, ρ_0 reflects the alloy scattering from the randomly distributed Si sites. As discussed above, the long-range order in Fe_3Si strongly depends on the Si content. Near stoichiometry, the layers are found to be ordered, and hence a decrease in the residual resistivity is observed. When randomly distributed Si atoms are added to pure Fe, the resistivity rapidly increases due to the enhancement of alloy scattering. The increase in the resistivity is suppressed for $x > 0.3$ when atomic ordering begins to occur. While the ordering is established, the resistivity turns from the local maximum at around $x=0.3$ to the minimum at the perfect ordering for stoichiometric Fe_3Si since in this case alloy scattering is strongly reduced and phonon scattering, which depends strongly on temperature, comes into play. For higher Si content or $x < 0$, the Si atoms replace the Fe atoms, randomly resulting in higher resistivity.

The effect of atomic ordering on saturation magnetization is shown in Fig. 3(b). As the Fe–Si composition is varied around stoichiometry, an excess of Fe will substitute into the Si sites, while any excess of Si replaces Fe in the sublattice B.[17] Thus the composition dependence of saturation magnetization (μ_B/cm^3) can be described by the following equation:

$$M_s = [(4+x)\mu_{\mathrm{Fe}}(B) + (4-x)\mu_{\mathrm{Si}}(D) + 8\mu_{\mathrm{eff}}(A,C)]/V, \tag{2}$$

where V denotes the volume of the unit cell, which is determined from the measured lattice constant. We use the magnetic moment of Fe at sublattice B $\mu_{\mathrm{Fe}}(B)=2.2\mu_B$ and the magnetic moment of Si at sublattice D $\mu_{\mathrm{Si}}(D)=-0.07\mu_B$. Fe at sublattices A and C has an average magnetic moment $\mu_{\mathrm{eff}}(A,C)$ that varies linearly with Fe concentration and has particular values of $1.35\mu_B$ for 75 at. % Fe and $2.2\mu_B$ for 100 at. % Fe.[17] The solid line in Fig. 3(b) shows the behavior of M_s according to Eq. (2), which qualitatively agrees with experiment for $x > 0.2$. For nearly stoichiometric samples, a significant decrease in saturation magnetization is observed in the experiment, which seems to be related to the finite disorder observed in HRXRD measurements. This behavior of M_s with composition is found to be different from the corresponding (001)-films, for which a linear behavior was observed.[19] This is most likely related to a different ordering in stoichiometric (113)-films.

We found the impact of ordering also in the earlier investigations of the so called PHE.[15] The PHE on [113]-oriented films exhibits an antisymmetric component, which is sensitive to the crystal symmetry,[15] and hence we examine the composition dependence of PHE in Figs. 3(c) and 3(d). The PHE on this orientation is the sum of a symmetric ρ_s^{113} and an antisymmetric component ρ_{SATM}.[15] The symmetric component ρ_s^{113} is negative for Fe and off-stoichiometric Fe_3Si samples and then increases with decreasing x. The behavior of the symmetric component is different compared to the [001]-oriented films,[20] which is because in [113]-films it corresponds to a different component of magnetoresistivity tensor.[15] Unlike the symmetric component, the antisymmetric component exhibits an identical sign for Fe and the nearly stoichiometric Fe_3Si films, which is expected because of the same crystal class for Fe and $D0_3$-ordered Fe_3Si.

In conclusion, we have studied structural, electrical, and magnetic properties of $Fe_3Si/GaAs(113)A$ hybrid structures dependent on the layer composition. The presence of superlattice reflections and lower resistivity confirms the long-range atomic ordering in the stoichiometric Fe_3Si films, reflecting the $D0_3$ crystal structure. A finite disorder was found even for the nearly stoichiometric films.

Part of this work has been supported by the German BMBF under the research program NanoQUIT (Contract No. 01BM463). The authors would like to thank B. Jenichen, O. Brandt, and M. Hashimoto for useful discussions and R. Ranchal for a critical reading of the manuscript.

[1] G. A. Prinz, Science **282**, 1660 (1998).
[2] T. J. Zega, A. T. Hanbicki, S. C. Erwin, I. Žutić, G. Kioseoglou, C. H. Li, B. T. Jonker, and R. M. Stroud, Phys. Rev. Lett. **96**, 196101 (2006).
[3] J. R. Waldrop and R. W. Grant, Appl. Phys. Lett. **34**, 630 (1979); H.-P. Schönherr, R. Nötzel, W. Ma, and K. H. Ploog, J. Appl. Phys. **89**, 169 (2001).
[4] J. Herfort, H.-P. Schönherr, A. Kawaharazuka, M. Ramsteiner, and K. Ploog, J. Cryst. Growth **278**, 666 (2005).
[5] Y. Hsieh, M. Hong, J. Kwo, A. Kortan, H. Chen, and J. Mannaerts, in *GaAs and Related Compound*, IOP Conference Proceedings Series No. 120, edited by G. B. Stringfellow (Institute of Physics, London, 1992), Vol. 154, p. 95.
[6] R. A. de Groot, F. M. Mueller, P. G. van Engen, and K. H. J. Buschow, Phys. Rev. Lett. **50**, 2024 (1983).
[7] J. Kudrnovsky, N. E. Christensen, and O. K. Andersen, Phys. Rev. B **43**, 5924 (1991).
[8] J. Herfort, H.-P. Schönherr, and K. H. Ploog, Appl. Phys. Lett. **83**, 3912 (2003).
[9] P. K. Muduli, J. Herfort, H.-P. Schönherr, and K. H. Ploog, J. Cryst. Growth **285**, 514 (2005a).
[10] A. Ionescu, C. A. F. Vaz, T. Trypiniotis, C. M. Gurtler, H. Garcia-Miquel, J. A. C. Bland, M. E. Vickers, R. M. Dalgliesh, S. Langridge, Y. Bugoslavsky, Y. Miyoshi, L. F. Cohen, and K. R. A. Ziebeck, Phys. Rev. B **71**, 094401 (2005).
[11] B. Jenichen, V. M. Kaganer, J. Herfort, D. K. Satapathy, H.-P. Schönherr, W. Braun, and K. H. Ploog, Phys. Rev. B **72**, 075329 (2005).
[12] F. Lin, D. Jiang, X. Ma, and W. Shi, Thin Solid Films **515**, 5353 (2007).
[13] T. Sadoh, H. Takeuchi, K. Ueda, A. Kenjo, and M. Miyao, Jpn. J. Appl. Phys., Part 1 **45**, 3598 (2006).
[14] M. Hansen, *Constitution of Binary Alloys* (McGraw-Hill, New York, 1958).
[15] P. K. Muduli, K.-J. Friedland, J. Herfort, H.-P. Schönherr, and K. H. Ploog, Phys. Rev. B **72**, 104430 (2005).
[16] V. Niculescu, K. Raj, J. I. Budnick, T. J. Burch, W. A. Hines, and A. H. Menotti, Phys. Rev. B **14**, 4160 (1976).
[17] W. A. Hines, A. H. Menotti, J. I. Budnick, T. J. Burch, T. Litrenta, V. Niculescu, and K. Raj, Phys. Rev. B **13**, 4060 (1976).
[18] W. B. Muir, J. I. Budnick, and K. Raj, Phys. Rev. B **25**, 726 (1982).
[19] J. Herfort, H.-P. Schönherr, K.-J. Friedland, and K. H. Ploog, J. Vac. Sci. Technol. B **22**, 2073 (2004).
[20] M. Bowen, K.-J. Friedland, J. Herfort, H.-P. Schönherr, and K. H. Ploog, Phys. Rev. B **71**, 172401 (2005).